DOI: 10.1002/ejic.200900084

Influence of Urea N–H Acidity on Receptor–Anionic and Neutral Analyte Binding in a Ruthenium(II)–Polypyridyl-Based Colorimetric Sensor

Amrita Ghosh,[a] Sandeep Verma,[b] Bishwajit Ganguly,*[a] Hirendra Nath Ghosh,*[b] and Amitava Das*[a]

Keywords: Ruthenium(II) complexes / Sensors / Urea / Ab initio calculations

A new ruthenium(II)–polypyridyl complex {$[Ru(bpy)_2\mathbf{L}]^{2+}$; bpy = 2,2′-bipyridyl, **L** = 1-(6-nitro-1,10-phenanthrolin-5-yl)-3-phenylurea} having a urea functionality as a receptor fragment for anionic analytes was synthesized. Its binding affinity towards various oxy anions and halides was studied. This complex was found to act as a selective colorimetric sensor for F^- among halides and $CH_3COO^-/H_2PO_4^-$ among oxy anions. The relative binding affinity of different anions towards this receptor was examined by using quantum chemical calculations. This complex was also found to act as a colorimetric sensor for neutral molecules like DMSO and DMF, though the binding affinity was weaker than that of the three anions mentioned above. The relative acidity of two HN_{urea} atoms was compared with that of one from the related complex by using pK_a calculations, and its influence on binding affinities towards different analytes is discussed. Results of the time-resolved fluorescence studies reveal that two nonequilibrated excited states exist involving two different ^{3}MLCT transitions, namely $Ru_{d\pi} \rightarrow bpy_{\pi^*}$ and $Ru_{d\pi} \rightarrow \mathbf{L}_{\pi^*}$.

Introduction

Anions, namely F^-, CH_3COO^- and $H_2PO_4^-$ are important in many biological processes and are known to be present in many commonly used agricultural fertilizers as well as in food additives.[1] These anions have been proven to have adverse effects on the environment.[2] Thus, the search for efficient chemosensors that can recognize and detect these anionic analytes has emerged as a major research area in current times.[3] A sensor molecule generally has a receptor component and a signalling unit that is capable of translating the analyte-binding induced changes into an output signal. This is generally probed either by spectroscopic techniques (e.g. fluorescence,[4] absorption and NMR spetroscopy) or by evaluating the change in redox potential values.[5,6] Among these, colorimetric sensors have a distinct advantage as they allow for visual detection of the targeted analyte through a change in colour.[3,5] Among various receptors, hydrogen-bond donor urea and thiourea functionalities have been widely used for selective binding of anions (A^-) like F^-, CH_3COO^- and $H_2PO_4^-$ through H-bonded adduct formation. The strength of this H bonding also depends on the relative acidity of the H atom ($HN_{urea/thiourea}$) of the urea and thiourea functionalities.[6c] There are examples where urea-based receptors, functionalized with electron-withdrawing groups, behave as a Brönsted acid in the presence of an excess of certain anions.[7–9] The high thermodynamic stability of HA_2^- is believed to govern this equilibrium process.[9a]

Neutral molecules like DMSO and/or DMF are important for their medicinal application or health hazard, and thus their recognition/sensing is crucial.[10] Further, developing a chemosensor for recognition of neutral molecules is even more challenging owing to the much weaker dipole–dipole or dipole–induced dipole interaction(s) as compared to the ion–dipole interaction that prevails for anionic analytes.[11] Earlier, an amide-based receptor was reported for DMSO where the association constant was found to be 160 M^{-1} at 295 K, where the binding phenomenon was probed through ^{1}H NMR spectroscopic studies.[11] For most urea-based receptors, owing to their limited solubility in common organic solvents, studies have been performed either in DMF or in DMSO as the solvent, and reports on the specific interaction of these molecules with urea functionalities in the solution phase is scarce.[12] There are a few examples where derivatives of organometallic compounds have been used as the signalling unit for anion recognition, and the receptor–anion binding phenom-

[a] Analytical Science Discipline, Central Salt and Marine Chemicals Research Institute (CSIR),
Bhavnagar 364002, Gujarat, India
Fax: +91-278-2567562
E-mail: ganguly@csmcri.org
amitava@csmcri.org
[b] Radiation and Photo Chemistry Division, Bhabha Atomic Research Centre,
Mumbai, India
E-mail: hnghosh@barc.gov.in

Supporting information for this article is available on the WWW under http://dx.doi.org/10.1002/ejic.200900084.

enon was probed through changes in redox potential, ^{1}H NMR chemical shifts or luminescence spectral patterns.[13,14] In most cases anion–receptor binding has failed to induce a significant change in the visible region of the spectra so that it allows for visual detection.

Herein, we have discussed how the presence of an electron-withdrawing functionality can actually influence the relative acidity of the H atom ($HN_{urea/thiourea}$) of the urea moiety and its consequential effect on the anion-binding affinity. Though there are many reports available in the literature describing the anion recognition phenomena and their possible implication in different applications, precise relationships between the acidity of the H-bond donor fragment and the relative affinity of a receptor towards different analytes are not addressed in detail.[9,13–15] The newly synthesized Ru^{II}–polypyridyl-based urea receptor **3** (Scheme 1) showed a detectable colour change on binding to analytes like F^-, among the halides, CH_3COO^- and $H_2PO_4^-$, among the oxy anions, and neutral molecules like DMSO and DMF; however, the extent of spectral changes was less for DMF and DMSO. Unlike receptor **2**,[16a] receptor **3** did not undergo deprotonation in the presence of an excess of anions, which was reflected in the partial quenching of the emission intensity in the presence of an excess of F^-, CH_3COO^- and $H_2PO_4^-$. In all cases, a 1:1 H-bonded adduct formation took place, and the respective association constant was evaluated from different spectral titration studies. The relative binding affinities of these anions with the receptor **3** were rationalized at the ab initio RHF/6-31G* level of theory and were compared with those of the related receptor **2**. Time-resolved emission studies further revealed the presence of two nonequilibrated $Ru_{d\pi} \rightarrow bpy_{\pi^*}/L_{\pi^*}$-based ^{3}MLCT excited states.

Results and Discussion

Urea functionality in complexes **2** and **3** was generated by treating 4-nitrophenyl isocyanate and phenyl isocyanate, respectively, with the pendant amino functionality of **1** in a dry acetonitrile/THF mixture (Scheme 1).[16a] Pure complexes were isolated through column chromatography, followed by a recrystallization process. All compounds were characterized by standard spectroscopic and analytical techniques.

In our earlier report we have shown that two different equilibriums exist for varying $[A^-]$ ($A^- = F^-$, CH_3COO^- and $H_2PO_4^-$) in the dry acetonitrile solution of receptor **2**; the first one being the H-bonded 1:1 adduct formation (**2**···A^- for $[A^-] < 1.5$ mol-equiv.) and the second one being the deprotonation equilibrium involving the HN_{urea} (–HN–CO–NH–) functionality, adjacent to the phen rather than the one adjacent to the nitrobenzene fragment (for $[A^-] > 1.5$ mol-equiv.).[16a] For complex **3** a change in the spectral pattern along with the associated detectable change in colour was observed when the acetonitrile solution of the tetrabutylammonium (TBA) salt of F^-, CH_3COO^- or $H_2PO_4^-$ (<2 mol-equiv.) was added to its acetonitrile solution; but no further change could be detected, neither in the spectral pattern nor in the colour of the solution on addition of a further excess (>2 to 100 mol-equiv.) of the respective anions. No colour change was noticed on addition of either Cl^-, Br^-, I^- or HSO_4^-, but a minor change in absorbance at around 350 nm was registered for Cl^- (Figure 1). These preliminary observations tend to suggest that unlike receptor **2**, equilibrium processes associated with the deprotonation of the urea functionality were absent for complex **3**.

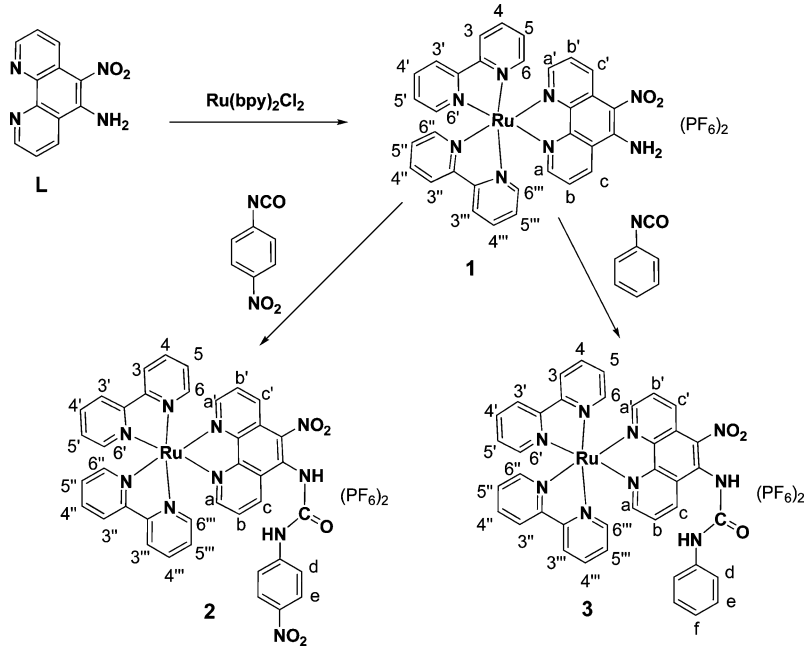

Scheme 1.

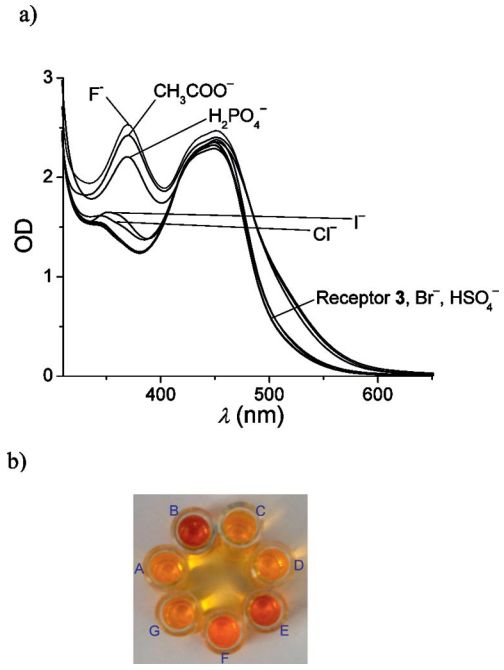

Figure 1. (a) Changes in UV/Vis spectra of receptor **3** (5.0×10^{-5} M) after the addition of different anions (ca. 5.0×10^{-4} M) in CH_3CN solution. (b) Respective colour changes for receptor **3** in the presence of various anions added in excess: A, receptor **3**; B, F^-; C, Cl^-; D, Br^-; E, CH_3COO^-; F, $H_2PO_4^-$; G, HSO_4^- (in acetonitrile).

To confirm this, a spectrophotometric titration for **3** in acetonitrile solution was carried out in the presence of varying $[A^-]$ ($A^- = CH_3COO^-$, $H_2PO_4^-$ or F^-) (Figure 2). Electronic spectra recorded for **3** in acetonitrile show absorption bands at 280, 340 and 455 nm, which were assigned as predominantly intraligand bpy/**L**-based $\pi \rightarrow \pi^*$, interligand bpy/**L**-based $\pi \rightarrow \pi^*$ and $Ru_{d\pi} \rightarrow bpy_{\pi^*}/\mathbf{L}_{\pi^*}$ transitions, respectively.[16b,17] The addition of the respective anions leads to a change in the absorption maxima from 343 to 372 nm, and a distinct shoulder appears within the wavelength range of 455–590 nm with two isosbestic points at around 298 and 412 nm. The appearance of two simultaneous isosbestic points signifies the presence of two different absorbing species that exist in equilibrium. Respective titration profiles [Figure 2(a)–(c)] and Benesi–Hildebrand plots (Supporting Information), shown as insets in Figure 2(a)–(c), reveal a 1:1 adduct formation in all cases. No further change in spectral patterns was observed, even in the presence of a large excess (100 mol-equiv.) of the added anions. The overall change in the spectral pattern of **3** was less than that for **2** for a comparable situation. All of this tends to suggest that the strong electron-withdrawing effect of the $-NO_2$ functionality on the benzene ring has an influence in governing the acidity of the –N–H proton in the urea moiety and thereby its affinity towards the respective anions and deprotonation phenomena. The inability of complex **3** to participate in the deprotonation equilibrium leads us to ascertain that the $-NO_2$ functionality present in the phen moiety does not contribute in enhancing the acidity of the H atom of the urea fragment. To confirm that the colour or spectral changes were solely due to the H-bonded adduct formation between A^- and the urea functionality, similar experiments were repeated with $Ru(bpy)_3^{2+}$. With $Ru(bpy)_3^{2+}$, no change in the spectral pattern on addition of the TBA salt of F^-, CH_3COO^- or $H_2PO_4^-$ was observed. This reveals that the urea functionality was responsible for binding to these anions. Reversible H-bonded adduct formation was also confirmed by adding little water to the acetonitrile solution of the respective adduct (**3**···A^-), while the spectra of the original compound was restored owing to the more effective solvation of these anions in water. The respective binding affinity of receptor **3** for three different anions was evaluated from the spectrophotometric titration and is shown in Table 1.

Experimentally obtained K_a values ($F^- > CH_3COO^- > H_2PO_4^-$) reflect the affinity of the conjugate base for protonation.[18] On the basis of our earlier studies it may be presumed that the broader absorption band at a longer wavelength arose predominantly from the bpy and **L**-based interligand charge-transfer transition,[16b] whereas the absorption band at around the 440–460 nm range is a combination of a predominantly $Ru_{d\pi} \rightarrow bpy_{\pi^*}/\mathbf{L}_{\pi^*}$ transition along with a certain contribution from the bpy and **L**-based interligand charge transfer.

$$\mathbf{3} + A^- \rightleftharpoons \mathbf{3}\cdots A^-;\ K_a$$

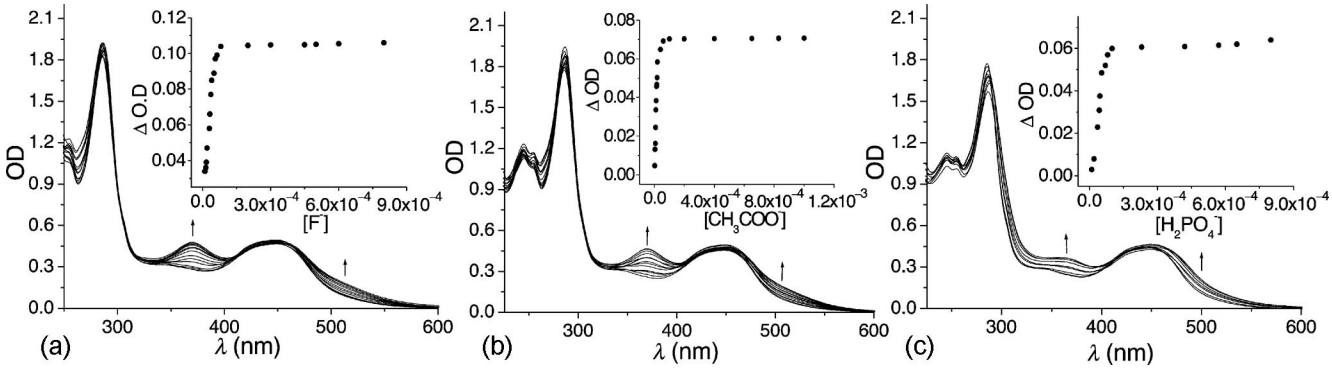

Figure 2. Electronic spectral response of receptor **3** (2.0×10^{-5} M) with varying $[A^-]$ in CH_3CN: (a) F^- (2.0×10^{-6} M to 1.0×10^{-4} M), (b) CH_3COO^- (2.0×10^{-6} M to 8.3×10^{-5} M), (c) $H_2PO_4^-$ (2.0×10^{-6} M to 8.1×10^{-5} M). Insets: Corresponding titration profile.

Table 1. Binding-constant values for the binding of different anions calculated from UV/Vis titrations.[a,b]

Anionic analyte	K_a ($\times 10^4$) [M^{-1}]	K_d ($\times 10^4$) [M^{-1}]
2···F^-[c]	22 (±1)	6.1 (±0.3)
2···CH_3COO^-[c]	19 (±2)	5.97 (±0.4)
2···$H_2PO_4^-$[c]	8.7 (±0.5)	1.2 (±0.1)
3···F^-	6.5 (±0.01)	–
3···CH_3COO^-	6.3 (±0.05)	–
3···$H_2PO_4^-$	1.4 (±0.03)	–

[a] Tetrabutyl salts of the respective anions were used for the studies. [b] The K value reported is the average of six independent data collections evaluated from individual UV/Vis titrations for the respective receptor and anion. Confidence limits for the respective K values are also shown. [c] Values are reported from ref.[16a]

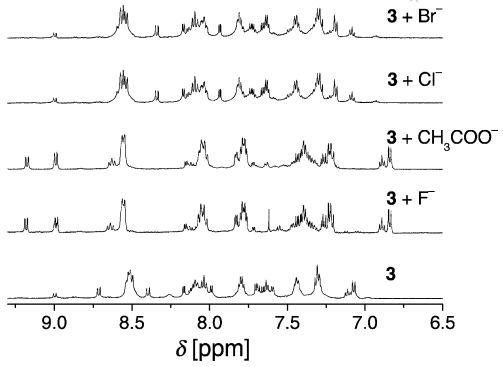

Figure 4. Partial ^1H NMR spectrum for **3** in the absence and presence of various anions in CD_3CN at 25 °C.

The emission spectra for receptor **3** were recorded in an air-equilibrated acetonitrile solution in the absence and presence of various anionic analytes and are shown in Figure 3.

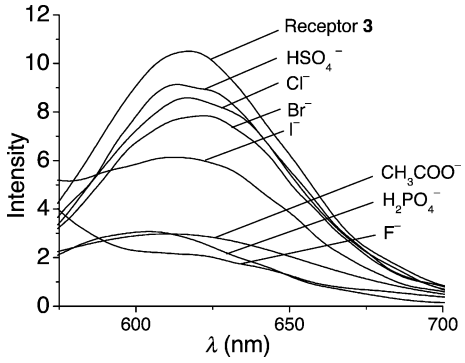

Figure 3. Emission spectra of receptor **3** (5.0×10^{-5} M) in the absence and presence of the respective anions (1.5×10^{-4} M) in acetonitrile solution.

Spectra for **3** show a characteristic emission band with λ_{max} at 616 nm on excitation of the $Ru_{d\pi} \rightarrow L_{\pi^*}/bpy_{\pi^*}$-based MLCT band at 449 nm. An appreciable quenching in emission intensity was observed on addition of 4 mol-equiv. of F^-, CH_3COO^- and $H_2PO_4^-$. The extent of quenching was much less when similar experiments were repeated with other anions (Figure 3). Complete luminescence quenching was observed when **2** was used as a receptor for identical studies, which was argued based on the deprotonation of the urea functionality.[16a] Therefore, results of the emission studies also corroborate with those from the absorption spectral studies.

To demonstrate the receptor–anion binding we recorded the ^1H NMR spectra for **3** in CD_3CN in the absence and presence of varying concentrations of anions. ^1H NMR spectra for **3** in the presence of an excess of the respective anion are shown in Figure 4. In CD_3CN no NH proton signal was observed for receptor **3**. Hence, we could only monitor the shifts of the aromatic proton signals.

A significant downfield shift for the H^c (Scheme 1) proton signal was observed upon addition of F^- and CH_3COO^-, with an upfield shift for the H^d proton signals. Such a downfield shift was not observed when other anionic analytes were added, and this signifies a very weak or negligible binding to the urea functionality. Binding constants for the 1:1 adduct formation (K_a) for F^- and CH_3COO^- were also confirmed from ^1H NMR spectroscopic titrations $\{K_a(F^-) = [6.3 \pm 0.1] \times 10^4$; $K_a(CH_3COO^-) = [6.01 \pm 0.1] \times 10^4\}$. Values thus obtained were close to those evaluated from spectrophotometric titrations (vide supra). For $H_2PO_4^-$, an insoluble complex was found to precipitate, and titration experiments could not be performed. A significant downfield shift of the H^c signal could be well explained from the quantum mechanical calculations, which is discussed in the following section (vide infra).

To rationalize the relative affinity of the receptor **3** towards various anionic analytes, ab initio quantum chemical calculations have been performed. For simplification we have used the phen–urea (**L**) moiety as a model for structure optimization. The structure of **L** and its complexes with F^-, Cl^-, Br^-, CH_3COO^-, $H_2PO_4^-$ and HSO_4^- were fully optimized at the Hartree–Fock HF/6-31G* level of theory.[8a,8b,16a] The computed receptor geometry for **L** and its corresponding complexes with the mentioned anions are shown in Figure 5.[19] For receptor **2**, this phen–urea moiety is designated as $\mathbf{L_1}$. The optimized structure for **L** and the corresponding complex with the anions F^-, CH_3COO^- or $H_2PO_4^-$ show a C–H···O-type interaction besides the complexing with the hydrogen atoms of the NH functionality of the urea moiety (Figure 5).

The C–H···O/C–H···X (X = halide) distance follows the order $F^- > CH_3COO^- > H_2PO_4^-$ (1.97, 2.24 and 2.33 Å, respectively) in these complexed forms. The oxy anions also show an interaction with the hydrogen atom H^c of the phen ring. This could account for the appreciable downfield shift of this proton signal in the ^1H NMR spectra. In the receptor **L**, the NH group adjacent to the phen fragment is intramolecularly H-bonded with the NO_2 group (Figure 5), however, it rotates while interacting with the anions. This results in the rupture of the intramolecular hydrogen bond in each case (Figure 5). The calculated binding energies (ΔE) were

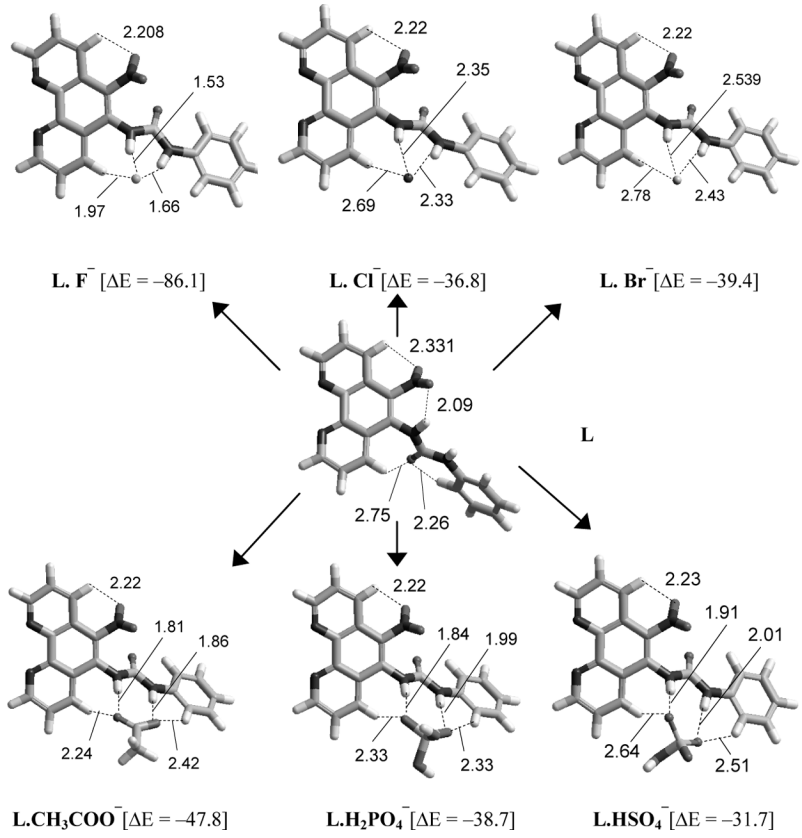

Figure 5. RHF/6-31G*-optimized geometries for **3** and its complexes with the F^-, Cl^-, Br^-, CH_3COO^-, $H_2PO_4^-$ and HSO_4^- anions along with the corresponding binding energies (ΔE in kcal/mol) given below each structure.

found to be in qualitative agreement with the observed trend obtained from the spectral behaviour (Table 1). Fluoride binds most effectively to **L** compared to other anions. Thus, the observed trend was in good agreement with the recent report on this type of anion sensor.[1c,16a,20] The binding affinity of Br^- with receptor **3** seems to be comparable to the binding affinity of the phosphate ion; however, the spectral change was not observed in the former case. It is difficult to explain this behaviour; presumably, the solvent effect might play a role in dictating the selectivity in these cases, which was not included in the calculations. By comparing the binding energies for receptors **2** and **3** with different anions, it is evident that **2** binds more strongly than **3** with different anions.[16a] It is worth noting that the deprotonation of receptor **2** takes place with an excess of these three anions. However, such deprotonation was not seen for the receptor **3**. To examine the relative acidity of the NH protons of the urea group of $\mathbf{L_1}$ and **L**, we have calculated the individual pK_a values of the respective urea moiety (Table 2).[21] Data presented in Table 2 show that the pK_a value for the NH proton of the simple urea is in close agreement with that of the experimentally obtained value (pK_a = 26.9).[22] The RHF-calculated pK_a value for urea is different from that of the experimental value; however, our interest was to examine the relative difference in pK_a values for the NH protons at different sites in $\mathbf{L_1}$ and **L**. These receptors are relatively larger in size, hence the computational simplicity, calculations were performed at the RHF level of theory. Table 2 shows that the pK_a values of $\mathbf{L_1}$ are smaller than those of receptor **L**, which suggests the higher acidity of the HN_{urea} protons for $\mathbf{L_1}$. This accounts for the observed deprotonation phenomena in $\mathbf{L_1}$ that was not observed for **L**. The calculated pK_a values helped us to distinguish the relative acidity of the two HN_{urea} protons of an individual receptor, one adjacent to the benzene group and the other one adjacent to the phen moiety.

Table 2. Calculated pK_a values for urea, receptor $\mathbf{L_1}$ and **L** in acetonitrile at the RHF/6-31G* level of theory. The B3LYP/6-311+G**-calculated value is in parentheses.

Compound		pK_a value
Simple urea		38.42 (24.22)
$\mathbf{L_1}$	deprotonation at NH adjacent to phenyl ring	30.51
	deprotonation at NH adjacent to phen	20.16
L	deprotonation at NH adjacent to phenyl ring	31.24
	deprotonation at NH adjacent to phen	25.72

Calculations show that for both compounds $\mathbf{L_1}$ and **L**, the HN_{urea} proton adjacent to the phen moiety has a lower pK_a value and is more acidic than the other one adjacent to the phenyl group. This result was found to be in agreement with the calculated structures for $\mathbf{L_1}$ and **L** with anionic analytes, which show that the HN proton adjacent to the phen moiety forms shorter H bonds with the F^- ion than the HN proton adjacent to the phenyl group (Fig-

ure 5). Presumably, the stability of the conjugate base formed from the deprotonation of the HN_{urea} proton adjacent to the phen moiety compared to HN proton adjacent to the phenyl group arises because of the attractive interaction between the nitrogen anion and the electron-deficient nitrogen atom of the nitro group (Supporting Information, Figure 3). Similar non-bonded attractive interactions have been reported.[23]

Binding Studies with DMSO and DMF

In our attempt to resolve the ^{1}H NMR spectroscopic signals for the urea protons in receptors **2** and **3**, the spectra for the respective receptors were recorded in [D_6]DMSO and [D_7]DMF. In both cases, broad and apparently downfield-shifted bands were observed. Further, the colour of the solution (either in DMF or DMSO) appeared to be different from that when acetonitrile was used as a solvent, and the associated colour change could be detected by the naked eye.

This indicated the possibility of a hydrogen-bonded adduct formation between the receptor (**2** and **3**) and the respective molecules DMSO or DMF. To the best of our knowledge, there are no reports on binding of the urea functionality to a neutral molecule. This offers the possibility of using these urea-based receptors as colorimetric sensors for neutral molecules like DMF and DMSO. However, to nullify the possibility of this spectral shift and the detectable colour change as a consequence of the shift of the charge-transfer transition band associated with the change in solvent polarity, we have recorded electronic spectra for these two compounds in solvents of varying polarity. No change was observed with any other solvent of comparable polarity. Thus, observed spectral changes in the presence of DMSO or DMF were certainly not the result of shifted charge-transfer bands in the presence of solvents of higher polarity and could be assigned to an H-bonded adduct formation. Electronic spectra for receptors **2** and **3** with varying [X] (X = DMSO or DMF) are shown in Figure 6. Systematic spectrophotometric titrations and associated ti-

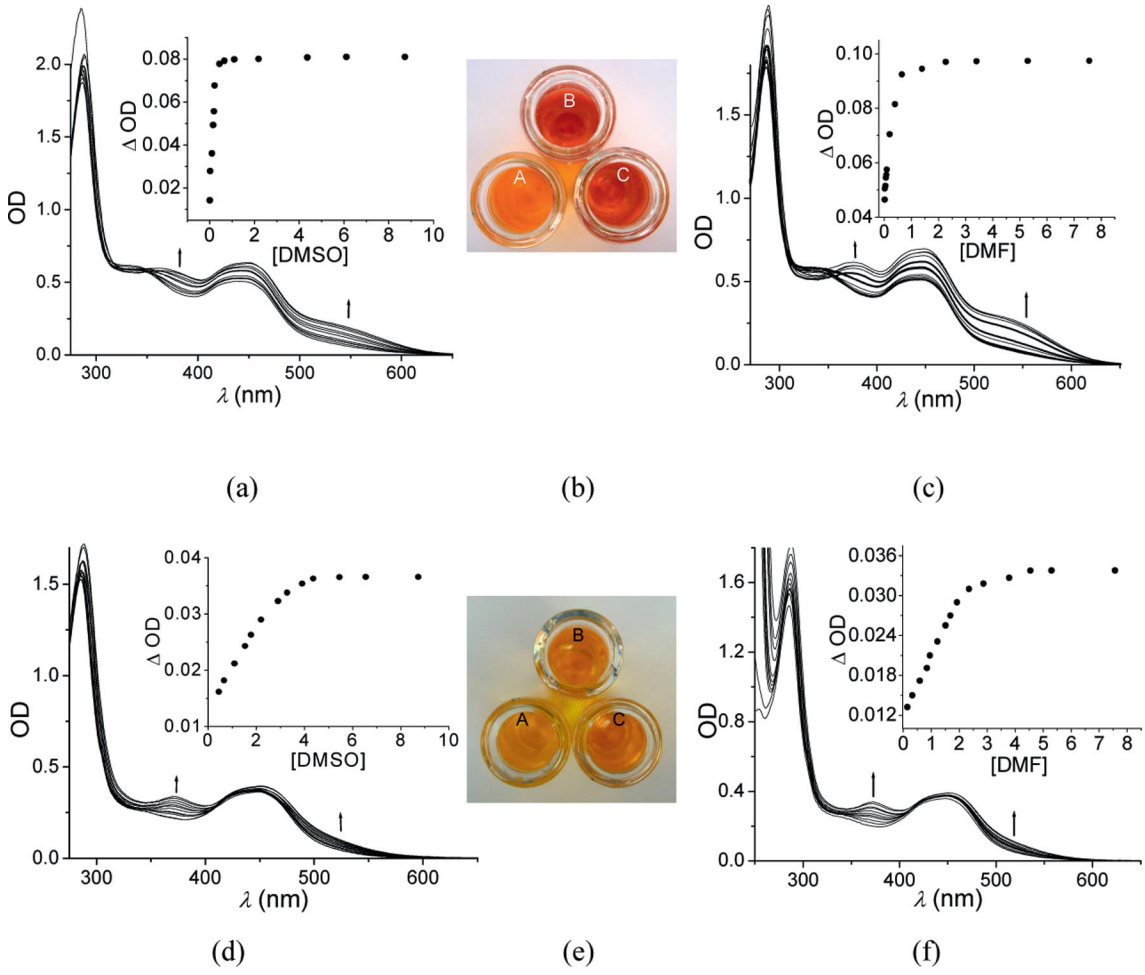

Figure 6. Absorption spectral titration of receptor **2** (2.0×10^{-5} M) and **3** (2.0×10^{-5} M) with DMSO, (a) and (d), [DMSO]: (1.3×10^{-2} to 0.6 M) with DMF, (c) and (f), [DMF]: (1.2×10^{-2} to 1.2 M); (b) and (e) show the corresponding colour changes for receptors **2** and **3**, respectively; **2** and **3**, (A); and DMSO, (B); and DMF, (C) for each compound. All the studies are performed in CH_3CN; insets: corresponding titration profiles for each titration.

tration profiles allow us to evaluate a 1:1 adduct formation along with the respective binding affinities (Table 3). Data presented in Table 3 clearly show that binding affinities of the respective receptors towards these neutral molecules are much weaker than they are with the anions. It may be mentioned here that these binding affinity values are comparable to the ones reported earlier by Smith et al., where an amide-based receptor synthesized in several steps was used for binding studies in ^{1}H NMR spectroscopic titrations.[13]

Table 3. Binding-constant values for DMSO and DMF calculated from UV/Vis spectroscopic titrations.[a]

Complex·DMSO/DMF	K_a ($\times 10^2$) [M^{-1}]
2·DMSO	1.86 (±0.2)
2·DMF	1.43 (±0.1)
3·DMSO	1.59 (±0.2)
3·DMF	1.04 (±0.1)

[a] The *K* value reported is the average of the six independent data collections taken from each UV/Vis titration for the respective receptor and anion. Confidence limits for the respective *K* values are also shown.

To have a better insight into the binding mode of DMSO and DMF to receptors **2** and **3**, geometries for these adducts were optimized at the RHF/6-31G* level of theory by using **L** and $\mathbf{L_1}$ as a model for Ru(bpy)$_2$**L**$^{2+}$ (Figure 7).

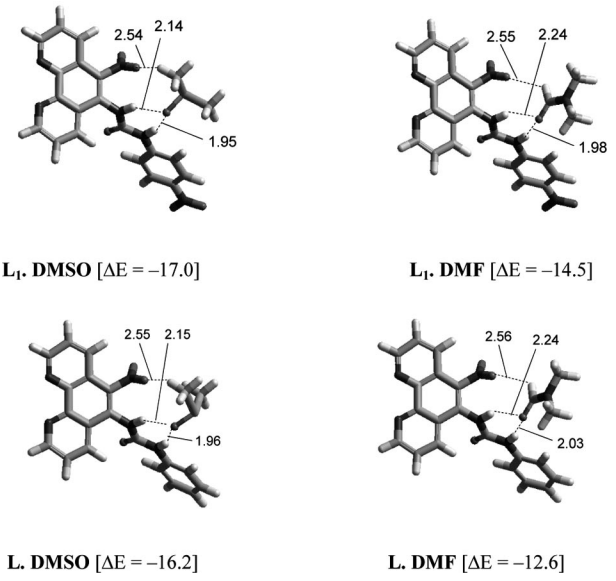

L_1. DMSO [ΔE = –17.0] **L_1. DMF** [ΔE = –14.5]

L. DMSO [ΔE = –16.2] **L. DMF** [ΔE = –12.6]

Figure 7. The RHF/6-31G*-optimized geometries for **2** and **3** and its complexes with DMSO and DMF with the corresponding binding energies given below each structure. Binding energies (ΔE) in kcal/mol.

The urea functionality of the parent structure for both receptors (**L** and $\mathbf{L_1}$) rotates when bound to different anions (Figure 5). However, in the case of the H-bonded adduct with DMSO or DMF no such rotation was observed, and an entirely different geometry for the respective adducts was obtained (Figure 7). The binding energy for DMSO/DMF is also found to be much lower than those for the halides/oxy anions and agrees well with the lower binding affinities that we have obtained experimentally (Table 3). Calculated binding energies further confirm stronger interactions of DMSO compared to DMF with these receptors (Figure 7).

Steady-state emission spectra for complexes **2** and **3** were recorded at room temperature in acetonitrile solution. Spectra for **3** show a broad emission band on excitation at 458 nm with λ_{max} at 617 nm, while that for complex **2** shows an emission band with λ_{max} at 620 nm. The broad emission band observed at around 620 nm for complexes **2** and **3** could be attributed to the $Ru_{d\pi} \rightarrow bpy_{\pi^*}/L_{\pi^*}$-based ^{3}MLCT excited state emission. Binding of the three anions to the receptors **2** and **3** is expected to cause an increase in the energy of the HOMO and a consequential narrowing of the HOMO–LUMO gap. This is expected to decrease the lifetime of the metastable ^{3}MLCT state and thereby the emission quantum yield. This was further confirmed by the time-resolved emission studies.

Luminescence decay traces for air-equilibrated acetonitrile solutions of complex **3** were monitored at 560 and 612 nm, following excitation with a 453 nm laser source. In both cases decay traces could be best fitted triexponentially with time constants τ_1 = 1.0 ns (79.2%), τ_2 = 5.6 ns (18.1%), τ_3 = 172 ns (2.7%) and τ_1 = 2.2 ns (16.0%), τ_2 = 9.0 ns (30%), τ_3 = 230 ns (54.0%), respectively (Figure 8). Earlier we observed that H-bond acceptor solvents (like DMSO and DMF) have some influence on the spectral behaviour owing to the H-bonded adduct formation **2**···X and **3**···X (X = DMSO or DMF). Acetonitrile is also known to participate in weak hydrogen-bond formation. Thus, to resolve the triexponential decay profile for complex **3** and the possibility of the excited state decay path associated with the H-bonded adduct with acetonitrile, we also recorded luminescence decay traces for complex **3** in benzene, a non-H-bonding solvent. Because of the limited solubility of this complex in benzene, a small fraction of acetonitrile was used (benzene/acetonitrile 99:1, v/v). Decay traces obtained for this solution at a monitoring wavelength of 560 nm and 612 nm with λ_{ext} = 453 nm could be best fitted by a single exponential and biexponential curves with time constants τ = 4.4 ns and τ_1 = 4.5 ns (95%), τ_2 = 187 ns (5%), respectively. This result led us to presume that emissions from two different states are actually involved in the excited states of complex **3**. In our earlier investigation with the Os(bpy)$_2$(**L**′)$^{2+}$ {**L**′ = [4-(3,4-dihydroxyphenyl)]-2,2′-bipyridyl} complex, two different emissive states were observed with different time constants of 9 ns and 34 ns.[24] The shorter one was attributed to the excited states involving substituted bipyridyl (**L**′), ($Ru_{d\pi} \rightarrow L'_{\pi^*}$) with a lower LUMO, and the longer one was attributed to the bpy-based ^{3}MLCT transitions ($Ru_{d\pi} \rightarrow bpy_{\pi^*}$). Similarly, in the present investigation the shorter component of 4.4 ns could be attributed to the emission lifetime associated with the $Ru_{d\pi} \rightarrow L_{\pi^*}$-based ^{3}MLCT excited state and the longer component to the $Ru_{d\pi} \rightarrow bpy_{\pi^*}$-based ^{3}MLCT excited state. This was further confirmed when we determined the emission lifetime for the air-equilibrated acetonitrile solution of

$Ru(bpy)_3^{2+}$, which showed a single exponential luminescence decay constant of 260 ns under identical conditions. However, the faster component (≤2.2 ns for λ_{mon} = 617 nm) that was observed at both wavelengths in acetonitrile was absent in a non-H-bonding solvent like benzene and could be attributed to the nonradiative deactivation process of the excited state through formation of a weak H-bond with surrounding solvent molecules. Similarly, faster and major components of the decay trace (1.0 ns, 79%) for **3** and (0.75 ns, 85.1%) **2** (λ_{mon} = 560 nm) could be best attributed to the deactivation of the excited state through a nonradiative pathway. Moreover, the presence of the strong electron-withdrawing functionality like NO_2 is expected to lower the **L***-based LUMO energy level. Perhaps these two effects together contributed to the overall faster decay constants for **2** compared to **3**. For comparison purposes we have carried out in detail the luminescence decay kinetics for **2** under identical conditions, and the kinetic decay trace was found to best fit to a triexponential function with typical time constants of τ_1 = 1.87 ns (38.3%), τ_2 = 16 ns (21.1%) and τ_3 = 171 ns (40.6%) (Figure 9). Among complexes **2** and **3**, the presence of an additional nitro functionality added to the higher acidity of the urea (N–H) protons (vide supra) and thereby to the more effective solvation of **2** in polar solvents. To examine the effect of anion binding to the receptor **3**, we studied the time-resolved luminescence decay profile in the presence of an excess of various anions, and decay traces are shown in Figure 10 and Table 4.

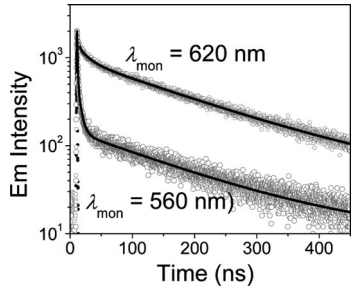

Figure 9. Luminescence decay kinetics for complex **2** at different monitoring wavelengths, following excitation at 453 nm in an air-equilibrated acetonitrile solution.

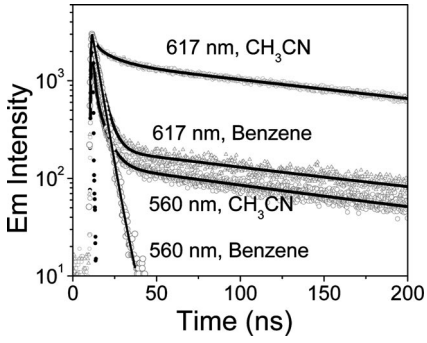

Figure 8. Luminescence decay kinetics for complex **3** at two different monitoring wavelengths 560 and 617 nm, following excitation at 453 nm in an air-equilibrated acetonitrile/benzene solution.

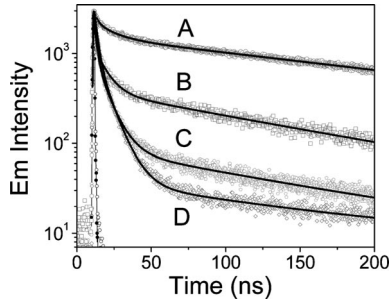

Figure 10. Luminescence decay kinetics for complex **3** in the absence (A) and presence of excess A^- [A^- = $H_2PO_4^-$ (B), F^- (C), CH_3COO^- (D)] following excitation at 453 nm (λ_{mon} = 617 nm) in an air-equilibrated acetonitrile solution.

Table 4. (A): Emission life times of receptors **2** and **3** in different air-equilibrated H-bonding solvents following excitation at 453 nm. (B): Emission life times of receptors **2** and **3** in different air-equilibrated acetonitrile solutions in the presence of different anions (excess).

A	Receptor **3**			
$\lambda_{monitor}$ [nm]	ACN	DMF	DMSO	
612	2.24 ns (27.1%)	1.2 ns (45.8%)	1.2 ns (67.6%)	
	12.9 ns (25.8%)	9.3 ns (20.1%)	7.6 ns (11%)	
	220 ns (47.1%)	222 ns (34.1%)	314 ns (21.4%)	
	Complex **2**			
620	1.87 ns (38.3%)	1.34 ns (59%)	1.0 ns (69.5%)	
	16 ns (21.1%)	13.5 ns (18.3%)	18.4 ns (12.7%)	
	171 ns (40.6%)	190 ns (22.7%)	244 ns (17.8%)	
B				
$\lambda_{monitor}$ [nm]	**3** + F^-	**3** + HPO_4^-	**3** + CH_3COO^-	**3**
617	1.5 ns (75.5%)	0.8 ns (75.3%)	2.08 ns (72.2%)	2.24 ns (27.1%)
	8.3 ns (22.5%)	7.9 ns (17.7%)	8.65 ns (27%)	12.9 ns (25.8%)
	128 ns (2%)	135 ns (7%)	134 ns (0.8%)	220 ns (47.1%)
	2 + F^-	**2** + HPO_4^-	**2** + CH_3COO^-	**2**
617	1.0 ns (76.6%)	0.7 ns (84.6%)	2.2 ns (72.9%)	1.87 ns (38.3%)
	8.0 ns (18.6%)	9.6 ns (8.1%)	8.9 ns (26.4%)	16 ns (21.1%)
	119 ns (4.8%)	120 ns (7.3%)	121 ns (0.7%)	171 ns (40.6%)

It is interesting to see that in the presence of different anions the contribution from the faster component differs significantly. In one of our recent reports,[16b] on the basis of detailed TD-DFT studies we have shown that for related Ru^{II}–polypyridyl complexes deprotonation or binding of the electron-rich anionic analyte to the receptor functionality, bound to the bpy derivative, caused an increase in the HOMO energy.

Thus, it will not be unreasonable to presume that a similar phenomenon will prevail here, which is expected to lower the HOMO–LUMO energy gap. According to the energy gap, law one would expect a faster decay of the excited triplet state owing to the narrowing of the energy gap between the excited triplet and ground singlet sate,[20] which is exactly what we have observed in the luminescence decay profiles in the presence of excess F^-; complex **3** + F^- (excess): [600 nm] τ_1 = 1.5 ns (75.5%); τ_2 = 8.3 ns (22.5%), τ_3 = 128 ns (2%) and for complex **2** + F^- (excess): [600 nm] τ_1 = 1.0 ns (76.6%); τ_2 = 8.0 ns (18.6%), τ_3 = 119 ns (4.8%). Decay traces for **3** in an acetonitrile solution in the presence of other anions are also shown in Figure 10.

As discussed earlier, a higher acidity of the H atoms of the NH_{urea} makes receptor **2** a better H-bond donor and thus forms a stronger H-bonded adduct with anionic analytes or H-bonding solvents. This accounts for the faster deactivation of the photo-excited ^{3}MLCT state associated with receptor **2** as compared to **3**. Further, in the presence of an excess of any of these three anions, **2** undergoes deprotonation, whereas **3** does not. Thus, for $\mathbf{2}_{-H^+}$, one would expect a more prominent effect on the HOMO energy as compared to that in **3**···A^-. To demonstrate the effect of the H-bond-accepting solvents on the excited-state lifetime for **3**, we recorded the luminescence decay profile in DMF and DMSO shown in Figure 11. Decay profiles were compared with those in acetonitrile as the solvent. For DMF and DMSO decay constants obtained for the 453 nm excitation (λ_{mon} = 620 nm) are as follows: τ_1 = 1.2 ns (45.8%), τ_2 = 9.3 ns (20.1%), τ_3 = 222 ns (34.1%) and τ_1 = 1.2 ns (75.5%); τ_2 = 7.6 ns (22.5%), τ_3 = 314 ns (2%), respectively. Spectral studies, discussed earlier, revealed a stronger H-bonded adduct formation for DMSO as compared to that of DMF with **3**. This is also evident in the faster decay profile for **3** in DMSO (Figure 11).

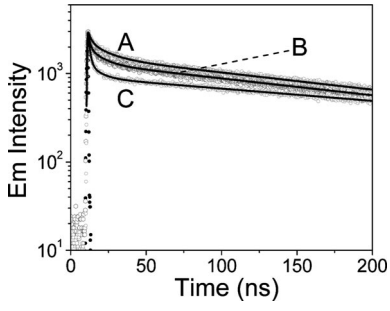

Figure 11. Luminescence decay kinetics for complex **3** in acetonitrile (A), DMF (B) and DMSO (C) following excitation at 453 nm (λ_{mon} = 617 nm) in air-equilibrated solutions.

Conclusions

We have synthesized a new Ru^{II}–polypyridyl complex with a pendant urea functionality, which could be used as a colorimetric sensor for certain anions like F^-, CH_3COO^- and $H_2PO_4^-$. Interestingly, this receptor works as a colorimetric sensor for neutral molecules like DMSO and DMF. The relative acidity of HN_{urea} hydrogen atoms was evaluated by pK_a calculations employing quantum chemical methods. Calculations reveal that the HN_{urea} proton close to the phen moiety is more acidic than that of the HN_{urea} hydrogen close to the phenyl group for both complexes **2** and **3**. The appearance of the broader absorption band for **2** and **3** and thereby their visual colour change, on binding to the anionic/neutral analyte, originated predominantly from the interligand charge transfer process involving bpy and $\mathbf{L}/\mathbf{L_1}$. Detailed time-resolved fluorescence studies revealed two nonequilibrated excited states based on two different ^{3}MLCT transitions, namely $Ru_{d\pi} \rightarrow bpy_{\pi^*}$ and $Ru_{d\pi} \rightarrow \mathbf{L}_{\pi^*}$, generated following excitation with a 440-nm laser source.

Experimental Section

Materials and Methods

Chemicals: $Ru(2,2'\text{-bpy})_2Cl_2{\cdot}2H_2O$ was prepared according to a literature procedure.[25] $RuCl_3{\cdot}xH_2O$, 2,2′-bipyridyl (bpy), 1,10-phenanthroline (phen), $[t\text{Bu}_4\text{N}]PF_6$, 4-nitrophenyl isocyanate and phenyl isocyanate were purchased from Aldrich Chemical Co. (USA) and were used as received. All solvents, used for synthesis, were dried and distilled before use according to standard procedures. Spectroscopic-grade solvents were used for all spectral and photophysical studies. 5-Nitro-1,10-phenanthroline, 6-amino-5-nitro-1,10-phenanthroline (**L**), $Ru(bpy)_2(\mathbf{L})(PF_6)_2$ (**1**)[26a] and $Ru(bpy)_2$[1-(6-nitro-1,10-phenanthrolin-5-yl)-3-(4-nitrophenyl)-urea]$(PF_6)_2$ (**2**)[16a] were synthesized according to literature procedures, and analytical data matched well with the proposed structure for $Ru(bpy)_2$[1-(6-nitro-1,10-phenanthrolin-5-yl)-3-phenylurea]-$(PF_6)_2$ (**2**).[26b]

Analytical Measurements: ^{1}H NMR spectra were recorded with either a Bruker 200 MHz FT NMR (model: Advance-DPX 200) or a Bruker 500 MHz FT NMR (model: Advance-DPX 500) spectrometer at room temperature (r.t., 25 °C). The chemical-shift (δ) data and coupling-constant (J) values are given in ppm and Hz, respectively throughout this manuscript unless mentioned otherwise. Tetramethylsilane (TMS) was used as an internal standard for all ^{1}H NMR spectroscopic studies. ESI-MS measurements were carried out with a Waters QTof-Micro instrument. Microanalyses (C, H, N) were performed by using a Perkin–Elmer 4100 elemental analyzer. Infrared spectra were recorded as KBr pellets by using a Perkin–Elmer Spectra GX 2000 spectrometer. UV/Vis spectra were obtained by using either a Shimadzu UV-3101 PC or a Cary 500 Scan UV/Vis/NIR spectrophotometer. Room-temperature steady-state emission spectra were obtained by using a Perkin–Elmer LS 50B luminescence spectrofluorimeter. The fluorescence quantum yields, ϕ_f, were estimated [Equation (1)] in appropriate solvents (as specified) by using the integrated emission intensity of $Ru(bpy)_3Cl_2$ (ϕ_f = 0.042 in H_2O at r.t.) as a reference:[27]

$$\phi_f = \phi_f' \, (I_{sample}/I_{std})(A_{std}/A_{sample})(\eta^2_{sample}/\eta^2_{std}) \quad (1)$$

where ϕ_f' is the absolute quantum yield for the $Ru(bpy)_3Cl_2$ complex, used as a reference; I_{sample} and I_{std} are the integrated emission intensities; A_{sample} and A_{std} are the absorbances at the excitation wavelength, and η^2_{sample} and η^2_{std} are the respective refractive indices.

Picosecond Time-Resolved Fluorimeter: Time-resolved fluorescence measurements were carried out by using a diode-laser-based spectrofluorimeter from IBH (UK). The instrument works on the principle of time-correlated single-photon counting (TCSPC).[28] In the present work, a 453-nm LED was used as the excitation light source, and a TBX4 detection module (IBH) coupled with a special Hamamatsu PMT was used for fluorescence detection.

Experimental Procedure

Synthesis of $Ru(bpy)_2$[1-(6-nitro-1,10-phenanthrolin-5-yl)-3-phenylurea]$(PF_6)_2$ (3): Complex **1** (150 mg, 0.164 mM) was dissolved in a minimum volume of acetonitrile. A solution of phenyl isocyanate (0.11ml, 1.0 mM) in freshly distilled and dried THF was added dropwise at room temperature through a dropping funnel to the solution of **1**. The whole reaction mixture was stirred under nitrogen for 48 h. The solvent was then evaporated under reduced pressure, and the crude solid thus obtained was subjected to column chromatography for purification. Neutral alumina (Grade III) was used as the stationary phase, and acetonitrile/toluene (1:1, v/v) was used as the eluent. The major fraction was collected and further purified by recrystallization from an acetonitrile/ether mixture. Yield 80 mg (44%). ^{1}HNMR (500 MHz, CD_3CN, TMS) δ = 8.71 (d, 1 H, J = 8.5 Hz, $H^{c'}$), 8.51 (t, 4 H, J = 6.5 Hz, H^5, $H^{5'}$, $H^{5''}$, $H^{5'''}$), 8.39 (d, 1 H, J = 8.5 Hz, H^c), 8.16 (d, 1 H, J = 5.0 Hz, $H^{a'}$), 8.09 (m, 2 H, H^e), 7.98 (d, 2 H, J = 6.5 Hz, $H^{6,6'''}$), 7.79 (d, 1 H, J = 5.0 Hz, H^a), 7.7–7.59 (m, 6 H, H^b, $H^{b'}$, H^4, $H^{4'}$, $H^{4''}$, $H^{4'''}$), 7.4 (m, 2 H, $H^{6'}$, $H^{6''}$), 7.31 (m, 4 H, H^3, $H^{3'}$, $H^{3''}$, $H^{3'''}$), 7.11 (t, 1 H, J = 7.5 Hz, H^f), 7.07 (t, 1 H, J = 7.5 Hz, H^d) ppm. FTIR (KBr): $\tilde{\nu}$ = 3328, 1650, 1597, 1545, 1495, 1443, 1313, 1232, 842 (br., PF_6), 755, 556, 762, 556 cm^{-1}. ESI-MS: m/z (%) = 1062 (ca. 2) [M^+], 917 (ca. 30) [$M^+ - PF_6$], 772 (ca. 20) [$M^+ - 2\ PF_6$]. $C_{39}H_{29}F_{12}N_9O_3P_2Ru$ (1062.7): calcd. C 44.08, H 2.75, N 11.86; found C 44.1, H 2.8, N 11.8.

Computational Details: All calculations were performed by using the GAMESS program suite.[29a] The theoretical calculations were performed by using the RHF/6-31G* basis set. For computational simplicity only the phenanthroline moiety was used as a model instead of the corresponding Ru^{II} complex **3** for studying the interaction with various anionic analytes. To calculate the pK_a values of the molecules we have considered the thermodynamic cycle shown below. The thermodynamic cycle yields in which the aqueous pK_a for the acid B–H is given by

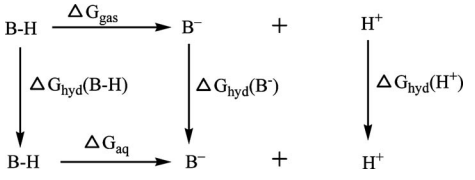

$$\Delta G_{aq} = \Delta G_{gas} + \Delta G_{hyd}(B^-) + \Delta G_{hyd}(H^+) - \Delta G_{hyd}(B\text{–}H).$$

At a given temperature T, the pK_a is then given by Equation (2).[29b]

$$pK_a = [G(B^-_{gas}) - G(BH_{gas}) + \Delta G_{hyd}(B^-) - \Delta G_{hyd}(BH) - 269.0]/1.3644 \quad (2)$$

The gas-phase free energy of protonation is calculated at the same level of theory as that used for the calculation of the solvation free energy. The free energy of solvation in water has been calculated by using SCRF (self-consistent reaction field) methods with the polarized continuum model (PCM).[29c–29f] A dielectric constant (ε) of 78.39 (water) was used in the solvation calculations, and the solvation-free energy of the proton taken from the experimental $\Delta G_{hyd}(H^+)$ value is equal to –259.0 kcal/mol. The values for $G(H^+_{gas})$ and $\Delta G_{hyd}(H^+)$ have been derived from experiments. We have used the values $\Delta G(H^+_{gas})$ = –6.28 kcal/mol and $\Delta G_{hyd}(H^+)$ = –264.61 kcal/mol. The calculation of G_{gas} uses a reference state of 1 atm, and the calculations of ΔG_{hyd} use a reference state of 1 M. Converting the ΔG_{gas} reference state (24.46 L at 298.15 K) from 1 atm to 1 M is accomplished by using Equation (3).

$$\Delta G_{gas}(1\ M) = \Delta G_{gas}(1\ atm) + RT\ln(24.46) \quad (3)$$

Spectrophotometric Titration: A 1.0×10^{-4} M solution of the respective complexes **2** and **3** in acetonitrile was prepared and stored under dark conditions. These solutions were used for all spectroscopic studies after appropriate dilution. 1.0×10^{-3} M solutions of tetrabutylammonium (TBA) salts of the respective anions were prepared in pre-dried and distilled acetonitrile and were stored under an inert gas. Solutions of complex **3** were further diluted for spectroscopic titrations, and the effective final concentration was adjusted to 2.0×10^{-5} M, while the final anionic analyte concentration for the titration was varied from 2.0×10^{-6} M to 1.0×10^{-4} M. Affinity constants were evaluated after calculating the concentrations of the respective species; free complex, A^- (A^- = F^-, $H_2PO_4^-$ or CH_3COO^-), X (X = DMSO or DMF) and associated complexes e.g. **3**···A^-, **2**···X or **3**···X (a 1:1 adduct of receptor **2** or **3** and A^- or X). The effect of the ionic strength on the affinity constant was also examined by repeating the studies at various (0–0.1 M [nBu$_4$N]-ClO_4) supporting electrolyte concentrations. Affinity constants were evaluated from a plot of a change in absorbance with varying analyte concentration at 540 nm, as the probe wavelength, and by using the equation $K_a = [\mathbf{L}A^-]/\{[\mathbf{L}]_{free}[A^-]_{free}\}$.

Luminescence Titration: The standard solutions used for the spectrophotometric titrations were also used for the luminescence titration studies. For all measurements λ_{ext} = 455 nm for the excitation wavelength. All titration experiments were performed by using 2.0×10^{-5} M solutions (air-equilibrated) of **2** and **3** in air-equilibrated acetonitrile solutions as the final and effective concentration, whereas final concentrations for anions were varied between 2.0×10^{-6} and 5.0×10^{-3} M.

Supporting Information (see footnote on the first page of this article): Emission and ^{1}H NMR titration spectra with various anions; optimized structure of the deprotonated form of **2**; mol ratio and Benesi–Hildebrand plot for the evaluation of the binding stoichiometry; results of the time-resolved studies of **3** in an acetonitrile solution.

Acknowledgments

The authors thank the Department of Science and Technology (India) for financial support. A. G. acknowledges the Council of Scientific and Industrial Research (CSIR) for a Sr. Research Fellow-

ship. A. D., B. G. and H. N. G. thank Dr. P. K. Ghosh (CSMCRI, Bhavnagar) and Dr. T. Mukherjee (BARC, Mumbai) for their keen interest in this work.

[1] a) K. Cammann, B. Ross, A. Katerkamp, J. Reinbold, B. Gründig, R. Renneberg, "Chemical and Biochemical Sensors" in *Ullman's Encyclopedia of Industrial Chemistry*, 6th ed., Wiley-VCH, New York, **1998**, DOI: 10.1002/14356007.b06_121; b) K. L. Krik, *Biochemistry of Halogens and Inorganic halides*, Plenum Press, New York, **1991**, p. 59l; c) A. Ghosh, A. Shrivastav, D. A. Jose, S. K. Mishra, C. K. Chandrakanth, S. Mishra, A. Das, *Anal. Chem.* **2008**, *80*, 5312; d) D. A. Jose, S. Mishra, A. Ghosh, A. Shrivastav, S. K. Mishra, A. Das, *Org. Lett.* **2007**, *9*, 1979; e) M. Suresh, D. A. Jose, A. Das, *Org. Lett.* **2007**, *9*, 441.

[2] a) K. Rurack, U. Resch-Genger, *Chem. Soc. Rev.* **2002**, *31*, 116; b) S. G. Tajc, B. L. Miller, *J. Am. Chem. Soc.* **2006**, *128*, 2532.

[3] a) E. Bianchi, K. Bowman-James, E. Garcia-Espana, *Supramolecular Chemistry of Anions*, Wiley-VCH, New York, **1997**; b) P. A. Gale, "Amide and urea based anion receptors", in *Encyclopedia of Supramolecular Chemistry*, Marcel Dekker, New York, **2004**, p. 31; c) C. Sukasai, T. Tuntulani, *Chem. Soc. Rev.* **2003**, *32*, 192; d) P. A. Gale, *Acc. Chem. Res.* **2006**, *39*, 465; e) R. Martinez-Manez, F. Sancenón, *Chem. Rev.* **2003**, *103*, 4419; f) A. P. De Silva, H. Q. N. Gunaratne, T. Gunnlaugsson, A. J. M. Hauxley, C. P. McCoy, J. T. Rademacher, T. E. Rice, *Chem. Rev.* **1997**, *97*, 1515; g) P. D. Beer, P. A. Gale, *Angew. Chem. Int. Ed.* **2001**, *40*, 486 and references cited therein; h) J. Yoon, S. K. Kim, J. Singh, K. S. Kim, *Chem. Soc. Rev.* **2006**, *35*, 355; i) T. Gunnlaugsson, M. Glynn, G. M. Tocci, P. E. Kruger, F. M. Pfeffer, *Coord. Chem. Rev.* **2006**, *250*, 3094.

[4] a) T. Gunnlaugsson, A. P. Davis, G. M. Hussey, J. Tierney, M. Glynn, *Org. Biomol. Chem.* **2004**, *2*, 1856; b) F. M. Pfeffer, M. Seter, N. Lewcenko, N. W. Barnett, *Tetrahedron Lett.* **2006**, *47*, 5241; c) J. Y. Lee, E. J. Cho, S. Mukamel, K. C. Nam, *J. Org. Chem.* **2004**, *69*, 943; d) G. Xu, M. A. Tarr, *Chem. Commun.* **2004**, 1050; e) C.-Y. Wu, M.-S. Chen, C.-A. Lin, S.-C. Lin, S.-S. Sun, *Chem. Eur. J.* **2006**, *12*, 2263.

[5] a) J. H. Hartley, T. D. James, C. J. Ward, *J. Chem. Soc. Perkin Trans. 1* **2000**, 3155; b) C. H. Lee, J. S. Lee, H. K. Na, D. W. Yoon, H. Miyji, W. S. Cho, J. L. Sessler, *J. Org. Chem.* **2005**, *70*, 2067; c) S. Mizukami, T. Nagano, Y. Urano, A. Odani, K. Kikuchi, *J. Am. Chem. Soc.* **2002**, *124*, 3920; d) F. Otón, A. Tárraga, M. D. Velasco, A. Espinosa, P. Molina, *Chem. Commun.* **2004**, 1658; e) P. Anzenbacher Jr, C. A. Try, H. Miyaji, K. Jursíková, V. M. Lynch, M. Marquez, J. L. Sessler, *J. Am. Chem. Soc.* **2000**, *122*, 10268.

[6] a) H. Lu, W. Xu, D. Zhang, D. Zhu, *Chem. Commun.* **2005**, 4777; b) D. Curiel, P. D. Beer, A. Cowley, M. R. Sambrook, F. Szemes, *Chem. Commun.* **2004**, 1162; c) Z.-B. Li, J. Lin, H.-C. Zhang, M. Sabat, M. Hyacinth, L. Pu, *J. Org. Chem.* **2004**, *69*, 6284; d) E. J. Cho, J. W. Moon, S. W. Ko, J. Y. Lee, S. K. Kim, J. Yoon, K. C. Nam, *J. Am. Chem. Soc.* **2003**, *125*, 12376; e) D. Curiel, A. Cowley, P. D. Beer, *Chem. Commun.* **2005**, 236.

[7] a) V. Amendola, D. Boiocchi, B. Colasson, L. Fabbrizzi, *Inorg. Chem.* **2006**, *45*, 6138; b) V. Amendola, D. Esteban-Gómez, L. Fabbrizzi, M. Licchelli, *Acc. Chem. Res.* **2006**, *39*, 343; c) Z.-H. Lin, S.-J. Ou, C.-Y. Duan, B.-G. Zhang, Z.-P. Bai, *Chem. Commun.* **2006**, 624; d) P. A. Gale, *Chem. Commun.* **2005**, 3761; e) S. Xu, K. C. Chen, H. Tian, *J. Mater. Chem.* **2005**, *15*, 2676; f) M. Boiocchi, D. L. Boca, D. Esteban-Gómez, L. Fabbrizzi, M. Licchelli, E. Monzani, *Chem. Eur. J.* **2005**, *11*, 3097; g) A. K. Evgeny, G. DanPantos, M. D. Reshetova, V. N. Khrustalev, V. M. Lynch, Y. A. Ustynyuk, J. L. Sessler, *Angew. Chem. Int. Ed.* **2005**, *44*, 7386; h) K. A. Nielsen, W.-S. Cho, J. Lyskawa, E. Levillain, V. M. Lynch, J. L. Sessler, J. O. Jeppesen, *J. Am. Chem. Soc.* **2006**, *128*, 2444 and reference cited therein; i) X. Peng, Y. Wu, J. Fan, M. Tian, K. Han, *J. Org. Chem.* **2005**, *70*, 10524; j) D. Esteban-Gómez, L. Fabbrizzi, M. Licchelli, *J. Org. Chem.* **2005**, *70*, 5717; k) Y. S. Lin, G. M. Tu, C. Y. Lin, Y. T. Chang, Y. P. Yen, *New J. Chem.*, DOI: 10.1039/b811172c.

[8] a) D. A. Jose, D. K. Kumar, B. Ganguly, A. Das, *Org. Lett.* **2004**, *6*, 3445; b) D. A. Jose, D. K. Kumar, B. Ganguly, A. Das, *Tetrahedron Lett.* **2005**, *46*, 5343; c) D. A. Jose, A. Singh, B. Ganguly, A. Das, *Tetrahedron Lett.* **2007**, *48*, 3695; d) D. E. Gomez, L. Fabbrizi, M. Licchelli, E. Monzani, *Org. Biomol. Chem.* **2005**, *3*, 1495; e) F. G. Bordwell, *Acc. Chem. Res.* **1988**, *21*, 456; f) J. Y. Kwon, N. J. Singh, H. Kim, S. K. Kim, J. Yoon, *J. Am. Chem. Soc.* **2004**, *126*, 8892; g) J. Y. Kwon, Y. J. Jang, S. K. Kim, K.-H. Lee, J. S. Kim, J. Yoon, *J. Org. Chem.* **2004**, *69*, 5155; h) Y.-J. Kim, H. Kwak, S. J. Lee, J. S. Lee, H. J. Kwon, S. H. Nam, K. Lee, C. Kim, *Tetrahedron* **2006**, *62*, 9635; i) T. Gunnlaugsson, A. P. Davis, J. E. O'Brien, M. Glynn, *Org. Lett.* **2002**, *4*, 2449; j) R. M. Duke, J. E. O'Brien, T. McCabe, T. Gunnlaugsson, *Org. Biomol. Chem.* **2008**, *6*, 4089; k) J. N. Babu, V. Bhalla, M. Kumar, R. K. Puri, R. K. Mahajan, *New J. Chem.*, DOI: 10.1039/b816610b; l) C. G. Gulgas, T. M. Reineke, *Inorg. Chem.* **2008**, *47*, 1548.

[9] a) T. Ghosh, B. G. Maiya, M. W. Wong, *J. Phys. Chem. A* **2004**, *108*, 11249; b) D. A. Jose, D. K. Kumar, P. Kar, S. Verma, A. Ghosh, B. Ganguly, H. N. Ghosh, A. Das, *Tetrahedron* **2007**, *63*, 12007; c) L. S. Evans, P. A. Gale, M. E. Light, R. Quesada, *Chem. Commun.* **2006**, 965; d) B. P. Hay, T. K. Firman, B. A. Moyer, *J. Am. Chem. Soc.* **2005**, *127*, 1810; e) V. S. Bryantsev, B. P. Hay, *J. Phys. Chem. A* **2006**, *110*, 4678; f) V. S. Bryantsev, B. P. Hay, *J. Am. Chem. Soc.* **2006**, *128*, 2035; g) M. Boiocchi, L. D. Boca, D. Esteban-Gómez, L. Fabbrizzi, M. Licchelli, E. Monzani, *J. Am. Chem. Soc.* **2004**, *126*, 16507; h) C. M. G. Santos, T. McCabe, T. Gunnlaugsson, *Tetrahedron Lett.* **2007**, *48*, 3135; i) C. M. G. dos Santos, T. McCabe, G. W. Watson, P. E. Kruger, T. Gunnlaugsson, *J. Org. Chem.* **2008**, *73*, 9235; j) P. Dydio, T. Zielinski, J. Jurczak, *J. Org. Chem.* **2009**, *74*, 1525.

[10] C. Redlich, W. S. Beckett, J. Sparer, K. W. Barwick, C. A. Riely, H. Miller, S. L. Sigal, S. L. Shalat, M. R. Cullen, *Ann. Intern. Med.* **1988**, *108*, 680–686; PMID 3358569: Liver disease associated with occupational exposure to the solvent dimethylformamide.

[11] C. Zhang, K. S. Suslick, *J. Am. Chem. Soc.* **2005**, *127*, 11548.

[12] a) E. M. Hampe, D. M. Rudkevich, *Tetrahedron* **2003**, *59*, 9619; b) S. Basurto, T. Torroba, M. Comes, R. Martınez, F. Sancenón, L. Villaescusa, P. Amoros, *Org. Lett.* **2005**, *7*, 5469; c) E. M. Hampe, D. M. Rudkevich, *Chem. Commun.* **2002**, 1450; d) C. Bucher, C. H. Devillers, J.-C. Moutet, G. Royal, E. Saint-Aman, *Chem. Commun.* **2003**, 888; e) R. Custelecean, B. A. Moyer, B. P. Hay, *Chem. Commun.* **2005**, 5971.

[13] a) I. V. Korendovych, R. A. Roesner, E. V. Rybak-Akimova, *Adv. Inorg. Chem.* **2007**, *59*, 109; b) M. J. Deetz, M. Shang, B. D. Smith, *J. Am. Chem. Soc.* **2000**, *122*, 6201; c) H. D. P. Ali, P. E. Kruger, T. Gunnlaugsson, *New J. Chem.* **2008**, *32*, 1153 and references cited therein; d) F. Otón, A. Espinosa, A. Tárraga, I. Ratera, K. Wurst, J. Veciana, P. Molina, *Inorg. Chem.* **2009**, *48*, 1566.

[14] C. R. Rice, *Coord. Chem. Rev.* **2006**, *250*, 3190.

[15] a) Y. Cui, H.-J. Mo, J.-C. Chen, Y.-L. Niu, Y.-R. Zhong, K.-C. Zheng, B.-H. Ye, *Inorg. Chem.* **2007**, *46*, 6427; b) T. Mizuno, W.-H. Wei, L. R. Eller, J. L. Sessler, *J. Am. Chem. Soc.* **2002**, *124*, 1134; c) Z. H. Lin, Y.-G. Zhao, C. Y. Duan, B. G. Zhang, Z. P. Bai, *Dalton Trans.* **2006**, 3678.

[16] a) A. Ghosh, B. Ganguly, A. Das, *Inorg. Chem.* **2007**, *46*, 9912; b) A. D. Jose, P. Kar, D. Koley, B. Ganguly, W. Thiel, H. N. Ghosh, A. Das, *Inorg. Chem.* **2007**, *46*, 5576; c) Z.-h. Lin, S.-j. Ou, C.-y. Duan, B.-g. Zhang, Z.-p. Bai, *Chem. Commun.* **2006**, 624; d) Z.-h. Lin, Y.-g. Zhao, C.-y. Duan, B.-g. Zhang, Z.-p. Bai, *Dalton Trans.* **2006**, 3678.

[17] F. Lachaud, A. Quaranta, Y. Pellegrin, P. Dorlet, M.-F. Charlot, S. Un, W. Leibl, A. Aukauloo, *Angew. Chem. Int. Ed.* **2005**, *44*, 1536.

[18] T. Steiner, *Angew. Chem. Int. Ed.* **2002**, *41*, 48.

[19] *Jaguar*, 5.5 ed.; Schrodinger, Inc, Portland, OR, **2004**.

[20] a) K. Choi, A. D. Hamilton, *Coord. Chem. Rev.* **2003**, *240*, 101; b) P. A. Gale, *Coord. Chem. Rev.* **2003**, *240*, 191; c) P. D. Beer, *Acc. Chem. Res.* **1998**, *31*, 71; d) J. L. Sessler, J. M. Davis, *Acc. Chem. Res.* **2001**, *34*, 989; e) J. H. Hartley, T. D. James, C. J. Ward, *J. Chem. Soc. Perkin Trans. 1* **2000**, 3155; f) C. R. Bondy, S. J. Loeb, *Coord. Chem. Rev.* **2003**, *240*, 77; g) M. Boiocchi, L. D. Boca, D. E. Gómez, L. Fabbrizzi, M. Licchelli, E. Monzani, *Chem. Eur. J.* **2005**, *11*, 3097.

[21] V. P. Kumar, B. Ganguly, S. Bhattacharya, *J. Org. Chem.* **2004**, *69*, 8634.

[22] a) F. G. Brodwell, *Acc. Chem. Res.* **1988**, *21*, 456; b) F. G. Brodwell, D. J. Algrim, J. A. Harrelson, *J. Am. Chem. Soc.* **1988**, *110*, 5903; c) E. Fan, S. A. Van Armon, S. Kincald, A. D. Hamilton, *J. Am. Chem. Soc.* **1993**, *115*, 369.

[23] K. Woniak, P. R. Mallinson, C. C. Wilson, E. Hovestreydt, E. Grech, *J. Phys. Chem. A* **2002**, *106*, 6897.

[24] S. Verma, P. Kar, A. Das, D. K. Palit, H. N. Ghosh, *J. Phys. Chem. C* **2008**, *112*, 7959.

[25] R. C. Young, T. J. Meyers, D. G. Whitten, *J. Am. Chem. Soc.* **1976**, *98*, 286.

[26] a) E. Ishow, A. Gourdon, J. P. Launey, C. Chiorboli, F. Scandola, *Inorg. Chem.* **1999**, *38*, 1504; b) ^{1}H NMR (200 MHz, CD_3CN, TMS,): δ = 8.63 (d, J = 8.2 Hz, 1 H, $H^{c'}$), 8.53 (t, J = 6.8 Hz, 4 H, H^5, $H^{5'}$, $H^{5''}$, $H^{5'''}$), 8.42 (d, J = 8.6 Hz, 1 H, H^c), 8.22 (d, J = 5.2 Hz, 1 H, $H^{a'}$), 8.11 (d, J = 9.4 Hz, 2 H, H^e), 8.02 (d, J = 7.6 Hz, 2 H, $H^{6,6'''}$), 7.81 (d, J = 5.2 Hz, 1 H, H^a), 7.75–7.61 (m, 6 H, H^b, $H^{b'}$, H^4, $H^{4'}$, $H^{4''}$, $H^{4'''}$), 7.6 (d, J = 7.2 Hz, 2 H, $H^{6'}$, $H^{6''}$), 7.42 (m, 4 H, H^3, $H^{3'}$, $H^{3''}$, $H^{3'''}$), 7.0 (d, J = 9.2 Hz, 2 H, H^d) ppm. FTIR (KBr): $\tilde{\nu}$ = 3573, 1596, 1539, 1503, 841 (br., PF_6), 762, 556 cm^{-1}. ESI-MS: m/z (%) = 985 (ca. 20) [$M^+ - PF_6 + Na^+$]. $C_{39}H_{28}F_{12}N_{10}O_5P_2Ru$ (1108): calcd. C 42.29, H 2.55, N 12.64; found C 42.3, H 2.6, N 12.56.

[27] A. Juris, V. Balzani, F. Barigelletti, S. Campagna, P. Belser, A. von Zelewsky, *Coord. Chem. Rev.* **1988**, *84*, 85.

[28] D. V. O'Connor, D. Phillips; *Time Correlated Single Photon Counting*, Academic Press, New York, **1984**.

[29] a) M. W. Schmidt, K. K. Baldridge, J. A. Boatz, S. T. Elbert, M. S. Gordon, J. H. Jensen, S. Koseki, N. Matsunaga, K. A. Nguyen, S. Su, T. L. Windus, M. Dupuis, J. A. Montgomery, *J. Comput. Chem.* **1993**, *14*, 1347 ("General Atomic and Molecular Electronic Structure System"); b) M. D. Liptak, G. C. Shields, *J. Am. Chem. Soc.* **2001**, *123*, 7314; c) J. Tomasi, M. Persico, *Chem. Rev.* **1994**, *94*, 2027; d) C. J. Cramer, D. G. Truhlar, *Solvent Effects and Chemical Reactivity* (Eds.: O. Tapia, J. Bertran), Kluwer Academic Publishers, Dordrecht, **1996**; e) S. Miertus, E. Scrocco, J. Tomasi, *J. Chem. Phys.* **1981**, *55*, 117; f) J. L. Pascual-Ahuir, E. Silla, J. Tomasi, R. Bonaccorsi, *J. Comput. Chem.* **1987**, *8*, 778.

Received: January 22, 2009
Published Online: May 11, 2009

